analytical chemistry

Article

pubs.acs.org/ac

Hollow-Channel Paper Analytical Devices

Christophe Renault, Xiang Li, Stephen E. Fosdick, and Richard M. Crooks*

Department of Chemistry and Biochemistry, Center for Nano- and Molecular Science and Technology, The University of Texas at Austin, 105 E. 24th Street Stop A5300, Austin, Texas 78712-1224, United States

Supporting Information

ABSTRACT: We present a microfluidic paper analytical device (μPAD) that relies on flow in hollow channels, rather than through a cellulose network, to transport fluids. The flow rate in hollow channels is 7 times higher than in regular paper channels and can be conveniently controlled from 0 to several mm/s by balancing capillary and pressure forces. More importantly, the pressure of a single drop of liquid (~0.2 mbar) is sufficient to induce fast pressure-driven flow, making hollow channels suitable for point of care diagnostics. We demonstrate their utility for simple colorimetric glucose and BSA assays in which the time for liquid transport is reduced by a factor of 4 compared to normal cellulose channels.

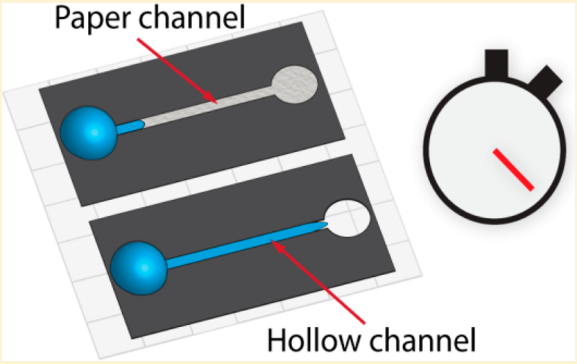

Here we report a microfluidic paper analytical device (μPAD) that relies on flow in hollow channels, rather than through a cellulose network, to transport fluids. The structural differences between hollow channels and paper channels are illustrated in Scheme 1. The important new result is that by removing the cellulose matrix from within a predefined channel and leaving the bottom of the channel hydrophilic, the flow rate of solution in the channel is enhanced by up to a factor of 7. There are several advantages to hollow-channel paper fluidic devices. First, no external equipment, such as a syringe pump, is required to force the liquid into the channel, which means that this type of hollow channel should be suitable for point-of-care (POC) applications.[1] Second, the high flow rate reduces analysis times and also makes it possible to use larger fluidic networks. Third, we hypothesize that removal of the cellulose from the channel will allow micrometer-sized objects, such as bacteria or microbeads, to flow freely. Fourth, the absence of the cellulose network should decrease nonspecific adsorption (NSA). In the present article we address the first two of these points, and in subsequent reports we will address the latter two.

Scheme 1

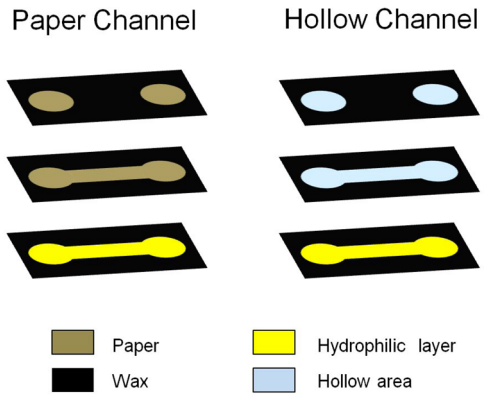

Dipsticks and lateral flow assays, such as the pregnancy test, are successful examples of paper-based diagnostic devices.[1,2] In 2007 the Whitesides group[3] reinvigorated this field by reporting μPADs based on two-dimensional paper patterns,[4] which enabled the fabrication of fluidic networks for multiplexing assays. Later, more dense fluidic networks were achieved by stacking multiple layers of paper with double-sided tape, leading to three-dimensional (3D) μPADs.[5] More recently, we introduced a simpler method for fabricating 3D μPADs, which is based on the principles of origami, and we showed that such devices (called oPADs) could perform complex operations.[6,7] In recent years a number of specific operations for increasing the functionality of 2D and 3D μPADs have been reported. These include flow timing,[8] sequential delivery of reagents,[9] and optical and electrochemical measurements.[10,11]

Despite the promise of paper as a platform for low-cost diagnostics, there are some important limitations. One of these is that the flow of liquids in porous paper channels is driven by capillary action,[12] and the distance penetrated by the liquid is proportional to the square root of time.[13] Consequently, fluid flow within cellulose channels is intrinsically slow. For example it takes ~15−20 min for water to wick through a typical 5 cm-long paper channel.[12] Long analysis times are not desirable, and they can lead to secondary problems such as solvent evaporation.[12] Indeed, slow flow in paper channels is one of

Received: June 14, 2013
Accepted: July 30, 2013
Published: August 9, 2013

the main reasons why nearly all 2D and 3D paper-based fluidic devices are relatively small (typically ~1−4 cm^2).

Our group recently reported one approach for constructing larger paper fluidic devices that can multiplex up to 285 assays without being compromised by the speed of fluid flow. We call the platform that enables this function a SlipPAD,[14] because it is based on the SlipChip concept originated by Ismagilov and co-workers.[15,16] The idea is that many reservoirs can be filled in parallel through connecting channels that are activated by slipping two wax-patterned paper fluidic layers relative to one another. Another example of rapid flow in a paper device was recently reported by Jahanshahi-Anbuhi et al.[17] Their approach involves channels fabricated using flexible films of polyethylene terephthalate, which results in a negative capillary pressure that pushes fluids. Finally, the Whitesides group has reported a method for increasing flow rates that involves removing the paper channel altogether.[18] Specifically, they cut a trench in thick cardstock paper, and then rendered the paper omniphobic by gas-phase reaction with fluoroalkyl siloxanes. Laminar flow was observed in this type of open-channel paper device, and various operations such as mixing, dilution, and droplet generation were achieved. These omniphobic channels are not wetted by water, however, and therefore a syringe pump is required to move fluids. In essence, this type of device is closely related to those based on poly(dimethylsiloxane).

In contrast to prior reports, we describe hollow channel-based *o*PADs that are very simple to fabricate, do not require a pump for operation, and that enable rapid fluid flow. These characteristics make them appropriate for POC diagnostics. We report the flow characteristics of these devices and then demonstrate their utility for simple colorimetric assays.

EXPERIMENTAL SECTION

Chemicals and Materials. Erioglaucine disodium salt was purchased from Acros Organics. Phosphate-buffered saline (PBS), 10X solution, 30% HCl, and Whatman grade 1 chromatographic paper were obtained from Fisher Scientific. Glucose oxidase (GOx) from *Aspergillus niger* (type X-S), peroxidase from horseradish (type VI) (HRP), D-(+)-glucose (referred to as glucose), and albumin from bovine serum (BSA) were purchase from Sigma-Aldrich. Tetrabromophenol blue was obtained from Alfa Aesar. Sodium citrate was provided by EM Science. KI was obtained from Mallinckrodt Specialty Chemicals Co., and ethanol (99.5%) was purchased from Pharmaco-Aaper. All solutions were prepared using deionized water (18.2 MΩ·cm, Milli-Q Gradient System, Millipore). All reagents were used as received without further purification.

Device Fabrication. *o*PADs were fabricated using a previously reported wax patterning method.[19,20] The devices were designed using CorelDraw12 software, and the specific patterns used for the different paper devices are provided in Supporting Information (Figure S1). Patterns were printed on Whatman chromatographic paper using a Xerox 8570DN inkjet wax printer. The paper was then placed in an oven at 120 °C for 1 min and then cooled to 20 °C. More details about the fabrication of the hydrophilic floor of the hollow channels will be provided in a forthcoming article.[21] The paper channels and reservoirs were cut using, respectively, a razor blade and a 4 mm inner-diameter punch (Harris Uni-core). Sharp tools are crucial to obtain a clean cut and to avoid clogging the channels.

Glucose and BSA Assays. For the glucose and BSA assays, the reagents were dried in paper reservoirs defined on the top layer of the device. Finally, the *o*PAD was folded according to the origami technique and tightly pressed together using two rigid 5 mm thick-polycarbonate pieces clamped with binder clips.

The glucose assay was prepared as follows. First, 1.0 μL of 0.86 M KI was drop casted into the paper wells. Second, after the KI solution was dried, 1.0 μL of a horseradish peroxidase/glucose oxidase solution (20/100 units) in phosphate-buffered saline solution (PBS) 1X (12 mM phosphate buffer, pH 7.4, 137 mM NaCl, and 2.7 mM KCl) was added to the wells. The BSA assay was prepared by drying 0.5 μL of a 250 mM citrate solution (sodium citrate solution acidified with concd HCl, pH 1.7) into each well, followed by addition of 0.5 μL of 3.3 mM tetrabromophenol blue in 95% ethanol. The solutions were dried at 20 °C under N_2. The glucose standards were prepared by diluting a glucose stock solution in PBS 1X buffer. The glucose stock solution was prepared 1 day before the experiment to allow the glucose to mutarotate. The BSA standards were also prepared in PBS 1X buffer.

An office scanner (HP C6180) was used to acquire optical images of the paper devices, and ImageJ freeware (NIH, Bethesda, MD) was used to analyze the colors. For the glucose assay, the color pictures were converted to grayscale, and then the average intensity was correlated to the concentration of glucose. For the BSA assay, each pixel of the picture was split into red, green, and blue color spaces. The color intensity of the red channel was correlated with the concentration of BSA.

RESULTS AND DISCUSSION

Fast Liquid Transport in Hollow Channels. The first part of this study focuses on the flow rate of an aqueous solution of a blue dye in a hollow channel as a function of time and pressure using the configuration shown in Figure 1a. The location of the dye was established by observing the passage of 5.0 mM aqueous erioglaucine past unwaxed 300 μm diameter paper windows defined along the hollow channel. The pressure

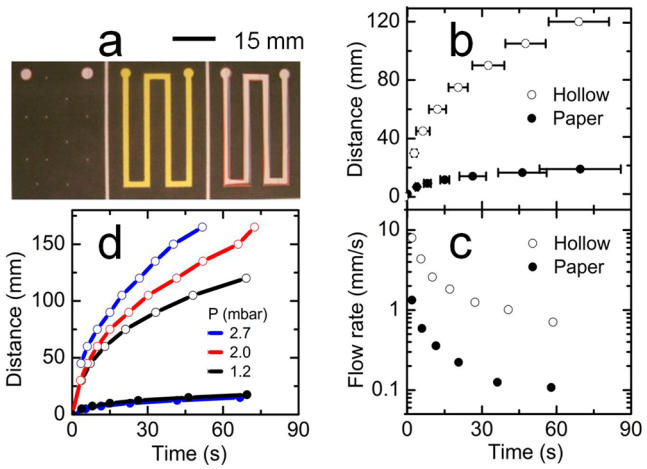

Figure 1. (a) Photograph of the unfolded *o*PAD used to measure flow rates. (b) Distance flowed by an aqueous 5.0 mM erioglaucine solution in a hollow channel (hollow circles) and a paper channel (filled circles) as a function of time. The error bars represent the standard deviation of four independent experiments. The hollow and paper channels were both ~180 μm tall by 2.5 mm wide. The pressure at the inlet was 1.2 mbar. (c) Flow rate calculated from the derivative of the data in Figure 1b. (d) Same experiment as (b) but with the indicated pressures at the inlet. The two superimposed curves for the paper channels were obtained at 1.2 and 2.7 mbar.

dx.doi.org/10.1021/ac401786h | *Anal. Chem.* 2013, 85, 7976−7979

was controlled by varying the height of the dye solution in the inlet reservoir. Because the height of the solution in the reservoir varies by a maximum of 10% during the time required to run experiments, the pressure was nearly constant for each measurement. The pressure P at the inlet was calculated using eq 1. Here ρ is the density of water

$$P = \rho \times g \times h \quad (1)$$

at 20 °C, g is the gravitational constant, and h is the height of the liquid in the inlet reservoir. To fully evaluate the performance of hollow channels, control experiments with paper channels were also carried out.

Figure 1b compares the distances traveled by an aqueous dye solution in hollow and paper channels during a 70 s time interval. The instantaneous flow rate, calculated as the derivative of distance as a function of time, is shown in Figure 1c. For both hollow and paper channels, the flow rate is not constant and decreases with time. However, the liquid flows much faster in the hollow channel. Indeed, during the 70 s duration of the experiment the flow rate in the hollow channel is on average 7 times higher than for the paper channel. This means that the dye travels about 12 cm in 70 s, compared to just 2 cm in the paper channel. Note that it takes about 1 h for the solution to flow 12 cm in a paper channel, and during this period evaporation of the sample can become a major problem.

The effect of the pressure on the flow rate is shown Figure 1d. The pressure at the inlet was varied from 1.2 to 2.7 mbar. Higher pressures lead to faster flow rates in hollow channels, but they have no effect on the flow rate in paper channels as demonstrated by the two superimposed curves (1.2 and 2.7 mbar) at the bottom of Figure 1d. More importantly, movie S1 (Supporting Information) shows that the pressure of a single drop of liquid, exerting ~0.2 mbar of pressure, is sufficient to fill a hollow channel. In fact, the pressure of a single drop is sufficient to fill a 1.5 cm long hollow channel in ~2 s while it takes 30 s to fill a paper channel having the same dimensions.

Although the high flow rates observed in hollow channels are primarily driven by pressure, capillary flow may also be important depending on the degree of hydrophobicity of the channel walls. Movie S2 (Supporting Information) shows that the paper floor of the hollow channel (yellow color in Scheme 1) is very hydrophilic while the wax walls are hydrophobic (water contact angle of 75°). Importantly, in the absence of a hydrophilic floor, aqueous solutions do not enter inside the hollow channel over the pressure range represented in Figure 1d (results not shown). This finding is consistent with results recently reported by Whitesides and co-workers,[18] wherein they use a syringe pump or relatively high pressures (~200 mbar, i.e., a column of water 2 m high) to drive fluids through hydrophobic paper channels. The hydrophilic floor is, therefore, key for enabling low-pressure (i.e., 0.2 mbar), high-speed flow through hollow channels.

As alluded to by the results presented thus far, the flow of liquids in hollow channels can be conveniently controlled by adjusting pressure and capillary forces. Indeed, in the absence of obstacles within the hollow channel, the liquid quickly reaches the outlet of the device and continues to flow until the inlet reservoir is empty (movie S3, Supporting Information). However, if there is a paper barrier within the hollow channel, the associated flow resistance can slow down the liquid, or stop it entirely, depending on the length of the barrier and the pressure at the inlet. For example, a 180 μm-long paper barrier placed at the inlet decreases the flow rate by a factor of 2 (compared to a barrier-free channel) under the influence of a 1.2 mbar pressure at the inlet. However, a 1 cm-long paper barrier completely stops the pressure-driven flow, leaving only the hydrophilic floor wet. Moreover, a 1 mm wide-hydrophobic wax line perpendicular to the hollow channel completely stops the liquid. The important point is that, in analogy to constrictions within other types of microfluidic devices,[22,23] wax lines and paper barriers can be used to control flow rates from between 0 and several mm/s. Photographs of the devices showing the precise location of the barriers used for the aforementioned experiments are provided in Figure S2 (Supporting Information).

Colorimetric Detection of Glucose and BSA. To demonstrate the potential of hollow channels for carrying out simple assays, we used glucose and BSA colorimetric reactions that have become commonplace for benchmarking paper fluidic devices.[3,5,24] The multiplexed assay was carried out using the 3D *o*PAD design shown in Figure 2a. The paper was prepared by drying the reagents for the glucose and BSA assays in the paper wells on the top layer of the device. The five wells on left and right were filled with the assay reagents for glucose and BSA, respectively. After the reagents were dried, the device was folded and an 80 μL drop of sample was introduced at the inlet located at center of the device. The hollow channel network shown Figure 2a directs the sample toward the two separate test zones. For both assays, the sample is split and delivered into each of five different wells to achieve five replicate results. Five minutes after the injection of the sample, excess liquid was removed from the inlet, and then the device was scanned to quantify the color change in the test wells.

A photograph of a paper device 5 min after injection of a sample containing 20 mM of glucose and 75 μM of BSA is shown Figure 2b. A change of color in both the glucose and

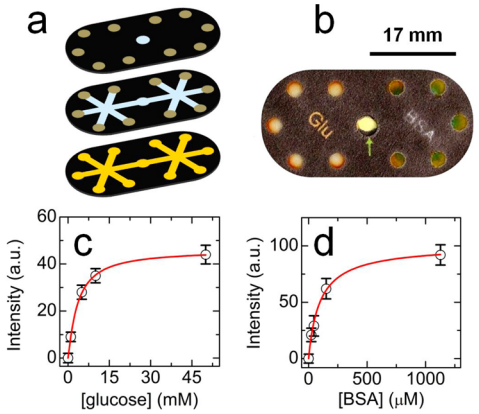

Figure 2. (a) Schematic representation of the *o*PAD used for the glucose and BSA assays. The color code is the same as that in Scheme 1. (b) Photograph of the glucose/BSA *o*PAD sensor. The picture was taken 5 min after introducing 80 μL of sample containing 75 μM BSA and 20 mM glucose in PBS 1X buffer. The color of the wells containing the glucose assay reagents turned from white to brown in presence of glucose. The color of the wells containing the BSA assay reagents turned from yellow to blue in presence of BSA. For intermediary concentrations of BSA the mixture of yellow and blue colors gives a green coloration to the wells. (c and d) Calibration curves for the glucose and BSA assays, respectively. The data were measured with two different devices, each one giving five replicates. The fitting parameters for the glucose and BSA calibration curves are provided in the Supporting Information.

dx.doi.org/10.1021/ac401786h | *Anal. Chem.* 2013, 85, 7976−7979

BSA testing wells is easily detected by the naked eye, which provides a means for making a quick semiquantitative reading. More importantly, however, quantitation can be achieved by analyzing the change of color using a desktop scanner. Samples containing different concentrations of glucose and BSA were used to calibrate the *o*PAD, and the resulting calibration curves for glucose and BSA are plotted in Figure 2c and 2d, respectively. A power function was used to fit the data, and the limits of detection (LODs) were found to be 0.7 mM for glucose and 18 μM for BSA. Details regarding the fitting of the calibration curves and the LOD calculations are provided in the Supporting Information.

For the *o*PAD assay described in the previous paragraph, it takes about 0.5 min for the sample to flow from the inlet to the reaction wells. For the 5 min total assay time, this leaves 4.5 min to develop the color in the test zones. For a paper device having a similar design, but paper rather than hollow channels, it takes ~2 min for the sample to reach the test zones. Thus, while sample transport accounts for only 10% of the total assay time in the hollow-channel *o*PAD, it consumes 40% of the assay time in a paper channel. Note that the more complex or multiplexed the assay, the more advantage there is to the hollow channels. Additionally, the larger-than-usual footprint of the *o*PAD used for the glucose and BSA assays (3.4 × 2.0 cm) is easier to handle than smaller paper-channel-based μPADs, which is an important point for some POC applications.

SUMMARY AND CONCLUSIONS

In this Article we have shown that hollow channels enable fluid transport in paper-based devices up to 7 times faster than in cellulose-containing channels. More importantly, the results indicate that pressure-driven flow is induced by a single drop of sample, thereby avoiding the need for pumping equipment. This point is crucial, because it enables the use of hollow channels for paper-based POC systems. Importantly, the flow rate within the hollow channels can be controlled by inserting hydrophobic weirs or short cellulose sections.

We have recently used paper-based *o*PADs having cellulose channels for DNA assays,[25] and in this application we have observed moderate to severe NSA even in the presence of blockers. Although the hollow channels reported here do have a cellulose floor, which is necessary to avoid the requirement for an external pump, we are optimistic that hollow channels will be useful for overcoming some of these NSA problems. Moreover, the open channels open up the possibility of using micrometer-scale objects either as assay components (microbeads, for example) or as targets (bacteria, for example). These are currently active areas of research in our group, and the results will be reported in due course.

ASSOCIATED CONTENT

Supporting Information

Details regarding chemicals and materials. Patterns used for *o*PAD designs. Movies of (1) an aqueous solution flowing in hollow and paper channels, (2) drop casting of an aqueous solution on the hydrophobic and hydrophilic walls of a hollow channel and (3) pressure-driven flow through a hollow channel. Photographs of paper devices containing paper and hydrophobic barriers along the hollow channel. Reaction pathways for the glucose and BSA assays. Procedure used for fitting the calibration curves and details regarding the calculation of LODs. This material is available free of charge via the Internet at http://pubs.acs.org.

AUTHOR INFORMATION

Corresponding Author

*Phone: 512-475-8674. E-mail: crooks@cm.utexas.edu.

Notes

The authors declare no competing financial interest.

ACKNOWLEDGMENTS

This project is sponsored by the Department of the Defense, Defense Threat Reduction Agency (contract number HDTRA-1-13-1-0031). The content of the information does not necessarily reflect the position or the policy of the federal government, and no official endorsement should be inferred. R.M.C. thanks the Robert A. Welch Foundation (Grant F-0032) for sustained research support.

REFERENCES

(1) Gubala, V.; Harris, L. F.; Ricco, A. J.; Tan, M. X.; Williams, D. E. *Anal. Chem.* **2011**, *84*, 487−515.
(2) Davies, R. J.; Eapen, S. S.; Carlisle, S. J. *Handbook of Biosensors and Biochips*; Wiley: Hoboken, 2008.
(3) Martinez, A. W.; Phillips, S. T.; Butte, M. J.; Whitesides, G. M. *Angew. Chem., Int. Ed.* **2007**, *46*, 1318−1320.
(4) Müller, R. H.; Clegg, D. L. *Anal. Chem.* **1949**, *21*, 1123−1125.
(5) Martinez, A. W.; Phillips, S. T.; Whitesides, G. M. *Proc. Natl. Acad. Sci. U.S.A.* **2008**, *105*, 19606−19611.
(6) Liu, H.; Crooks, R. M. *J. Am. Chem. Soc.* **2011**, *133*, 17564−17566.
(7) Liu, H.; Xiang, Y.; Lu, Y.; Crooks, R. M. *Angew. Chem., Int. Ed.* **2012**, *51*, 6925−8.
(8) Lutz, B. R.; Trinh, P.; Ball, C.; Fu, E.; Yager, P. *Lab Chip* **2011**, *11*, 4274−8.
(9) Fu, E.; Lutz, B.; Kauffman, P.; Yager, P. *Lab Chip* **2010**, *10*, 918−20.
(10) Carrilho, E.; Phillips, S. T.; Vella, S. J.; Martinez, A. W.; Whitesides, G. M. *Anal. Chem.* **2009**, *81*, 5990−5998.
(11) Dungchai, W.; Chailapakul, O.; Henry, C. S. *Anal. Chem.* **2009**, *81*, 5821−5826.
(12) Schilling, K. M.; Lepore, A. L.; Kurian, J. A.; Martinez, A. W. *Anal. Chem.* **2012**, *84*, 1579−1585.
(13) Washburn, E. W. *Phys. Rev.* **1921**, *17*, 273−283.
(14) Liu, H.; Li, X.; Crooks, R. M. *Anal. Chem.* **2013**, *85*, 4263−4267.
(15) Du, W.; Li, L.; Nichols, K. P.; Ismagilov, R. F. *Lab Chip* **2009**, *9*, 2286−2292.
(16) Li, L.; Ismagilov, R. F. *Annu. Rev. Biophys.* **2010**, *39*, 139−58.
(17) Jahanshahi-Anbuhi, S.; Chavan, P.; Sicard, C.; Leung, V.; Hossain, S. M. Z.; Pelton, R.; Brennan, J. D.; Filipe, C. D. M. *Lab Chip* **2012**, *12*, 5079−5085.
(18) Glavan, A. C.; Martinez, R. V.; Maxwell, E. J.; Subramaniam, A. B.; Nunes, R. M. D.; Soh, S.; Whitesides, G. M. *Lab Chip* **2013**.
(19) Lu, Y.; Shi, W.; Jiang, L.; Qin, J.; Lin, B. *Electrophoresis* **2009**, *30*, 1497−500.
(20) Carrilho, E.; Martinez, A. W.; Whitesides, G. M. *Anal. Chem.* **2009**, *81*, 7091−7095.
(21) Renault, C.; Koehne, J.; Ricco, A. J.; Crooks, R. M. Three Dimensional Wax Patterning of Paper Fluidic Devices. *Anal. Chem.*, to be submitted for publication.
(22) Chatterjee, D.; Mansfield, D. S.; Anderson, N. G.; Subedi, S.; Woolley, A. T. *Anal. Chem.* **2012**, *84*, 7057−7063.
(23) Yang, J.; Li, C.-W.; Yang, M. *Lab Chip* **2004**, *4*, 53−59.
(24) Dungchai, W.; Chailapakul, O.; Henry, C. S. *Anal. Chim. Acta* **2010**, *674*, 227−33.
(25) Scida, K.; Li, B.; Ellington, A.; Crooks, R. M. DNA detection using origami paper analytical devices. *Anal. Chem.*, to be submitted for publication.